EMARO + M1
EUROPEAN MASTER ON ADVANCED ROBOTICS

MASTER CORO M1
MASTER COMMANDE ET ROBOTIQUE
MASTER IN CONTROL AND ROBOTICS

Project Report

June 26, 2018

Determination of the Wrench Feasible Workspace of a 2-dof Tensegrity Manipulator

Wanting JIN
Xirui LIU

Supervisors

Philippe Wenger (Philippe.Wenger@ls2n.fr)
Matthieu Furet (matthieu.furet@ls2n.fr)

Contents

Chapter 1

Introduction

The report introduces our work on the project of determination of the wrench feasible workspace of a 2-dof tensegrity manipulator. We used the given kinematic and dynamic model of the manipulator to generate the workspace and explore an appropriate way to describe the workspace. Our work is mainly done by using Matlab.

1.1 Introduction of 2-dof tensegrity manipulator

A tensegrity structure is an assembly of compressive elements (bars) and tensile elements (cables, springs) held together in equilibrium with one or several elements are actuated[1],[3]. Tensegrity is known in architecture and art for more than a century [2], [4] and is suitable for modelling living organisms [4]. In our case, the two degree of freedom planar tensegrity manipulator is assembled by two Snelson's X-shape mechanism which is a crossed four-bars mechanism with springs along each lateral side,see Figure 1.1.

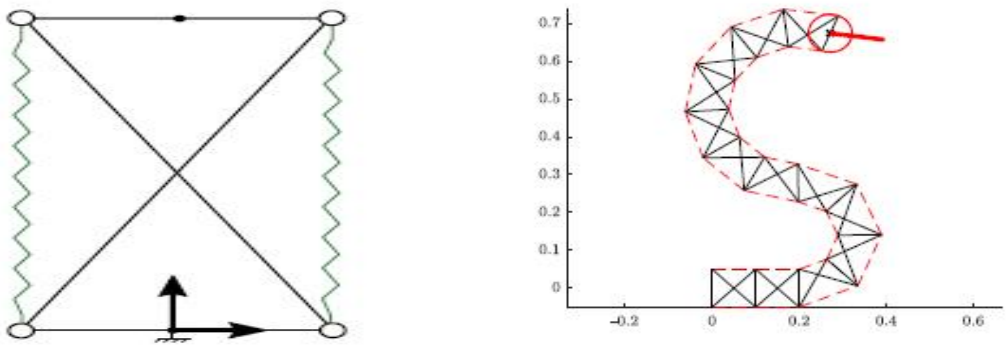

Figure 1.1: Single X-mechanism and assembled bird neck mechanism by several X-mechanism

The manipulator can be driven by two cables through the springs. To actuate the manipulator, we have several different actuation schemas to apply. In order to simplify our problem, we set two rotatory motors which are located on the both ends of the first bottom bar to actuate the manipulator since it only has two degree of freedom in planar. Furthermore, if the stiffness of the mechanism need to be controlled, more motors are acquired.[3]

1.2 Introduction of the method of determining workspace

The reachable workspace of the manipulator can be generated from the geometric model in which we don't take into account any limit of the actuation. Moreover, in our case, the actuation wrench of the tensegrity manipulator which is cable-driven is limited and the wrench feasible workspace(WFW) is introduced.
The pose of the tensegrity manipulator is said to be wrench feasible, if the tension forces in the cables can counteract any external wrench that applied to the end-effector. The WFW is defined as the set of poses that are wrench feasible. It must respect the kinematic constraint, static equilibrium and the limit of actuation wrench.
Generally, three methods are used to study the workspace of the manipulator: Graphical method, analytical method and numerical method. Graphical method directly gives the cross-section of the workspace. It is intuitive but not suitable for complex manipulator. Analytical method uses the equation of the boundary of the workspace. It is hard to obtain the boundary equation and the equation can be extremely complex. Numerical method uses large amount of joint variable pairs to generate a point cloud of the workspace. The accuracy of the workspace is depend on the amount of joint variable pairs. This method can be applied to any kind of manipulator and it is easy to code. The only drawback is that there is a clear trade-off between the accuracy and the time cost. In our case, we use the point cloud which is generated through numerical method to describe the workspace of the manipulator.

Chapter 2

Kinematic analysis

A single X-mechanism is a four-bar structure with crossed links and has two elastic springs. The bottom bar of a module is fixed to the upper bar of the formal module. The bottom bar of the first module is fixed to the ground[1]. In our case, two rotatory motors are needed and they are placed on the each side of the first module's bottom bar. The motors can only apply forces on the each side on upper bars through the two tendons which run through the springs, see Figure 2.1. The length of each springs

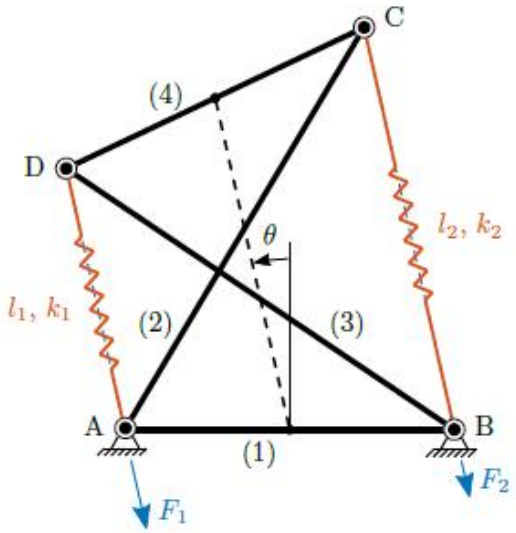

Figure 2.1: The first module consisting bars, tendons and springs

are denoted as l_1 and l_2 with the corresponding spring stiffness k_1 and k_2. We denote the length between the middle point of bottom bar(Link 1) and upper bar(Link 4) as l. The angle between l and the normal of Link 1 is denoted as θ. ϕ denotes the angle between Link 2 and Link 1. ψ denotes the angle between Link 3 and Link 1.
We can directly obtain the loop-closure equations from the structure.

$$\begin{cases} b + Lcos(\psi) + bcos(2\theta) - Lcos(\phi) = 0 \\ Lsin(\psi) + bsin(2\theta) - Lsin(\phi) = 0 \end{cases} \tag{2.1}$$

Then, from the loop-closure equation 2.1, we can use θ to express ψ and ϕ.

$$\begin{cases} \psi = 2arctan(-2bLsin(2\theta) + 2(\sqrt{(b^2L^2sin(2\theta)^2 + b^2L^2(cos(2\theta)+1)^2 - b(cos(2\theta)+1)^4)} \\ \qquad , 2b(cos(2\theta)+1)^2 - 2bL(cos(2\theta)+1)); \\ \phi = 2arctan(2bLsin(2\theta) + 2(\sqrt{(b^2L^2sin(2\theta)^2 + b^2L^2(cos(2\theta)+1)^2 - b(cos(2\theta)+1)^4)} \\ \qquad , 2b(cos(2\theta)+1)^2 + 2bL(cos(2\theta)+1)) \end{cases} \tag{2.2}$$

And the length of springs are expressed as:

$$\begin{cases} l_1 = \sqrt{b^2 + L^2 + 2bLcos(\psi)} \\ l_2 = \sqrt{b^2 + L^2 - 2bLcos(\phi)} \end{cases} \tag{2.3}$$

One module has 1 degree of freedom which means the geometric configuration of the module can be expressed uniquely by one variable θ. Without loss of generality, the workspace of each mechanism is calculating with respect to the middle point of the upper bar.
Generally, to make the module symmetric, we assume that:

(1) The springs have the same original length l_0, stiffness k and no mass.

(2) The crossed bar(Link 2 and Link 3) have the length L, the bottom bar(Link 1) and upper bar(Link 4) have the same length b and L should always greater than b.

(3) The range of θ is limited in $[-\frac{\pi}{2}, \frac{\pi}{2}]$.

(4) There is no friction and damping.

Then, we studied the 2-dof tensegrity manipulator which consists two identical X-mechanism as shown in Figure 2.2.

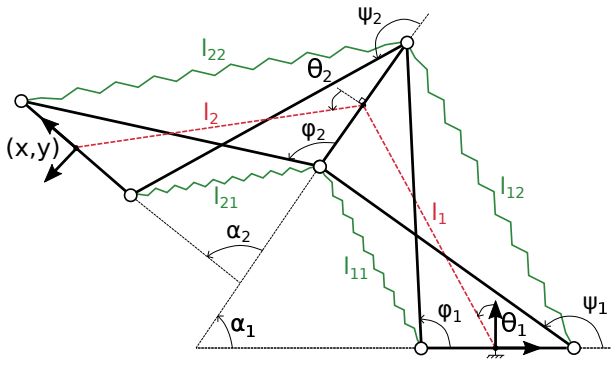

Figure 2.2: 2-dof tensegrity manipulator description

α denotes the angle between Link 4 and Link 1. Due to the symmetrical design, we can directly got the relationship: $\alpha = 2\theta$. And the direct kinematic equations are:

$$l_i(\theta_i) = \sqrt{L^2 - b^2 cos^2(\theta_i)} \tag{2.4}$$

$$\begin{cases} x = -l_1(\theta_1)sin(\theta_1) - l_2(\theta_2)sin(2\theta_1 + \theta_2) \\ y = l_1(\theta_1)cos(\theta_1) + l_2(\theta_2)cos(2\theta_1 + \theta_2) \end{cases} \tag{2.5}$$

Then, we calculated the Jacobian Matrix between Δx and $\Delta\theta$.

$$\Delta x = J\Delta\theta \tag{2.6}$$

$$J = \begin{bmatrix} -sin(\theta 1)^2 * b^2 * cos(\theta 1)/l_1 - l_1 * cos(\theta 1) - 2 * l_2 * cos(2 * \theta 1 + \theta 2), \\ -sin(2 * \theta 1 + \theta 2) * b^2 * cos(\theta 2) * sin(\theta 2)/l_2 - l_2 * cos(2 * \theta 1 + \theta 2); \\ cos(\theta 1)^2 * b^2 * sin(\theta 1)/l_1 - l_1 * sin(\theta 1) - 2 * l_2 * sin(2 * \theta 1 + \theta 2), \\ cos(2 * \theta 1 + \theta 2) * b^2 * cos(\theta 2) * sin(\theta 2)/l_2 - l_2 * sin(2 * \theta 1 + \theta 2) \end{bmatrix} \tag{2.7}$$

Chapter 3

Dynamic analysis

In this chapter, we will use dynamic analysis to introduce a proper actuation strategy. In chapter 2, we mentioned that the 2-dof tensegrity manipulator needs two motors to actuate and the actuation strategy should respect the geometric constraints, static equilibrium and actuating force limitation[3].
Expect from the constraints that we mentioned in chapter 2, we have more constraints when actuating the manipulator. Since the forces is applied to the end-effector through cables, we can only pull the cables which means the forces must be positive. Of course, the maximum force is limited due to the maximum torque that the actuators can supply. So, we have the range of force:

$$0 \leq F \leq F_{max} \tag{3.1}$$

And for a single spring, the length should be in the range of $[L-b, L+b]$. In our case, the spring should never be compressed, so the original length of the spring should in the range of $[0, L-b]$.That is because if the springs are compressed, they will supply pushing forces and the mechanism will become unstable. From the perspective of energy, the static equilibrium position corresponds to the minimum energy. Since we are considering the static case, the kinetic energy is 0 and only the potential energy is considered. As a planar manipulator, we can ignore the gravity potential energy. We only take the elastic potential energy of the cables and springs into account. The elastic potential energy of the cables and the springs are shown in Equation 3.2 and 3.3.

$$U_{cables} = F_1(l_{11} + l_{21}) + F_2(l_{12} + l_{22}) \tag{3.2}$$

$$U_{spring} = \frac{1}{2}(k_{11}(l_{11} - l_0)^2 + k_{12}(l_{12} - l_0)^2 + k_{21}(l_{21} - l_0)^2 + k_{22}(l_{22} - l_0)^2) \tag{3.3}$$

The total potential energy is given below:

$$U_{total} = U_{cables} + U_{springs} \tag{3.4}$$

By calculating the partial derivative of the potential energy U_{total} to joint configurations $[\theta_1, \theta_2]$ respectively, we can obtain the relationship between the actuating forces and

the joint configurations when a static equilibrium is reached.

$$\begin{cases} \dfrac{\partial U_{total}}{\partial \theta_1} = 0 \\ \dfrac{\partial U_{total}}{\partial \theta_2} = 0 \end{cases} \tag{3.5}$$

$$\begin{cases} a(\theta_1)F_1 + b(\theta_1)F_2 = c(\theta_1) \\ a(\theta_2)F_1 + b(\theta_2)F_2 = d(\theta_2) \end{cases} \tag{3.6}$$

Then, we can solve the binary equation of F_1 and F_2 by using equation 2.2 and 2.3.

$$\begin{cases} F_1 = \dfrac{b(\theta_1)d(\theta_2) - c(\theta_1)b(\theta_2)}{a(\theta_1)b(\theta_2) - a(\theta_2)b(\theta_1)} \\ F_2 = \dfrac{a(\theta_1)d(\theta_2) - c(\theta_1)a(\theta_2)}{a(\theta_1)b(\theta_2) - a(\theta_2)b(\theta_1)} \end{cases} \tag{3.7}$$

with:

$$\begin{cases} a(\theta) = \dfrac{b^2 cos(\theta) sin(\theta)}{\sqrt{L^2 - b^2 cos^2(\theta)}} - b cos(\theta) \\ b(\theta) = \dfrac{b^2 cos(\theta) sin(\theta)}{\sqrt{L^2 - b^2 cos^2(\theta)}} + b cos(\theta) \\ c(\theta_1) = -(k_{11}(\sqrt{L^2 - b^2 cos^2(\theta_1)} - b sin(\theta_1) - l_0)a(\theta_1)) \\ \qquad\quad +(k_{12}(\sqrt{L^2 - b^2 cos^2(\theta_1)} + b sin(\theta_1) - l_0)b(\theta_1)) \\ d(\theta_2) = -(k_{21}(\sqrt{L^2 - b^2 cos^2(\theta_2)} - b sin(\theta_2) - l_0)a(\theta_2)) \\ \qquad\quad +(k_{22}(\sqrt{L^2 - b^2 cos^2(\theta_2)} + b sin(\theta_2) - l_0)b(\theta_2)) \end{cases} \tag{3.8}$$

From the equation 3.7 and 3.8, we can find some interesting things. When $\theta_1 = \theta_2$, the denominator of F_1 and F_2 become 0 and F_1 and F_2 are infinite which exceeded the limit of forces, as shown in equation 3.1.

In next chapter, we will discuss the relationship between the forces and the workspace.

Chapter 4

Generate approximate wrench feasible workspace

To analyse the workspace of a tensegrity manipulator, we should first consider the kinematic constraints that associated to the geometric structure of the manipulator and the static equilibrium with minimum potential energy as well. Thus, to determine the configuration of the end-effector of a tensegrity manipulator is more complex than the ones of a rigid manipulator due to the tension parts(springs and cables). When we consider the static equilibrium, we can see that the end-effector configuration and the internal forces are coupled which means the external wrench effects internal forces as well as the end-effector configuration. Therefore, the external wrench should be taken into account when generating the workspace. The definition of wrench feasible workspace will be given in following section.

4.1 Wrench feasible workspace

The definition of workspace is related the conditions to be fulfilled at each point in the workspace. For the reachable workspace, the only condition that needs to be met is the kinematic constraint which is provided by the geometric structure.
For the wrench feasible workspace, it needs to meet the static equilibrium condition and the actuating forces limitation as well, shown in equation 3.5 and 3.1. Thus, the definition of wrench feasible workspace of the tensegrity manipulator is given as: the set of all end-effector configurations for which, if the tension forces in the tension parts can counteract any feasible set of external wrench that applied to the end-effector[5]. In our case, the feasible set of external wrench means the set of actuating forces which respect to the limitation. The tension forces of the springs can counteract the external wrenches means the static equilibrium is achieved, shown in equation 3.4 and 3.5.
To generate the wrench feasible workspace, the general idea is to find the pair of $F1$ and $F2$ corresponding to one specified end-effector configuration, then check if the pair of $F1$ and $F2$ is within the limitation of actuating force. If so, we call the

specified end-effector configuration is wrench feasible configuration. All the set of wrench feasible end-effector configuration compose the wrench feasible workspace.
As written in chapter 1, the numerical method is the most appropriate way to generate the wrench feasible workspace for our case. Thus, in the next two sections, we will discuss two approaches to apply numerical method to find wrench feasible configuration.

4.2 Sampling from Cartesian space

In this section, we sample from Cartesian space which means given the position of end-effector (x, y) to calculate corresponding F. Since we already knew the relationship between (F_1, F_2) and (θ_1, θ_2) in equation 3.7, we still need to find the relation between (x, y) and (θ_1, θ_2) where the inverse kinematic model is required.
As we know that the wrench feasible workspace is a subset of reachable workspace, we can roughly estimate the range of the reachable workspace to determine the sample range of (x, y). Thus, we take the circumscribed rectangle of the reachable workspace as the sample range. Then, for each sample point (x, y), we use inverse kinematic model to calculate corresponding joint configuration (θ_1, θ_2). It is worthy to note that there probably exists more than 1 joint configuration solution for one pair of (x,y). We restored all the solution and calculate corresponding (F_1, F_2). We can say that the specified (x,y) is in the WFW if there exists at least one pair of IGM solution(θ_1, θ_2) with corresponding (F_1, F_2) are within the limit of actuating forces. The set of all the wrench feasible (x, y) compose the WFW. There is an obvious advantage of this method is that we directly sample from Cartesian space which means the sample density of the WFW is even. Obviously, the smaller sample interval, the more points are evaluated and the more accuarcy of the WFW. As we applied this method to matlab, we found that for calculating IGM and corresponding F once,the average cost is about 0.18 second. As we set 40000 sample points, the total time cost is very high which means the method of sampling from cartisian space is not suitable.

4.3 Sampling from joint space

In this section, we sample from joint space (θ_1, θ_2), and calculate corresponding (F_1, F_2), then check the actuating forces limit condition, if so calculate direct kinematic equation and generate WFW. Different from sampling from Cartisian space, we don't need to calculate inverse geometric this time. It shorten the calculating time significantly which means we can have more sample points and obtain higher accuracy.

4.3.1 Discretization of joint configuration

To sample from joint space, we can directly discrete the joint configuration which is easy to implement in Matlab. As we already knew the limit of θ_1 and θ_2, we can discretize the range into N parts, where N is the number of samples. Totally, we need to calculate N^2 times the corresponding forces. Of course, the larger value of N, the more accuracy of WFW.
However, there still remains some problem. When we apply direct geometric model which is an injection function, the sample points are not distributed evenly in wrench feasible workspace as shown in equation 2.6 and 2.7.
It may leads to some situation that there are quite a lot of wrench feasible points which are located in a quite small region. We call it high density of the distribution of wrench feasible points as shown in figure 4.1.

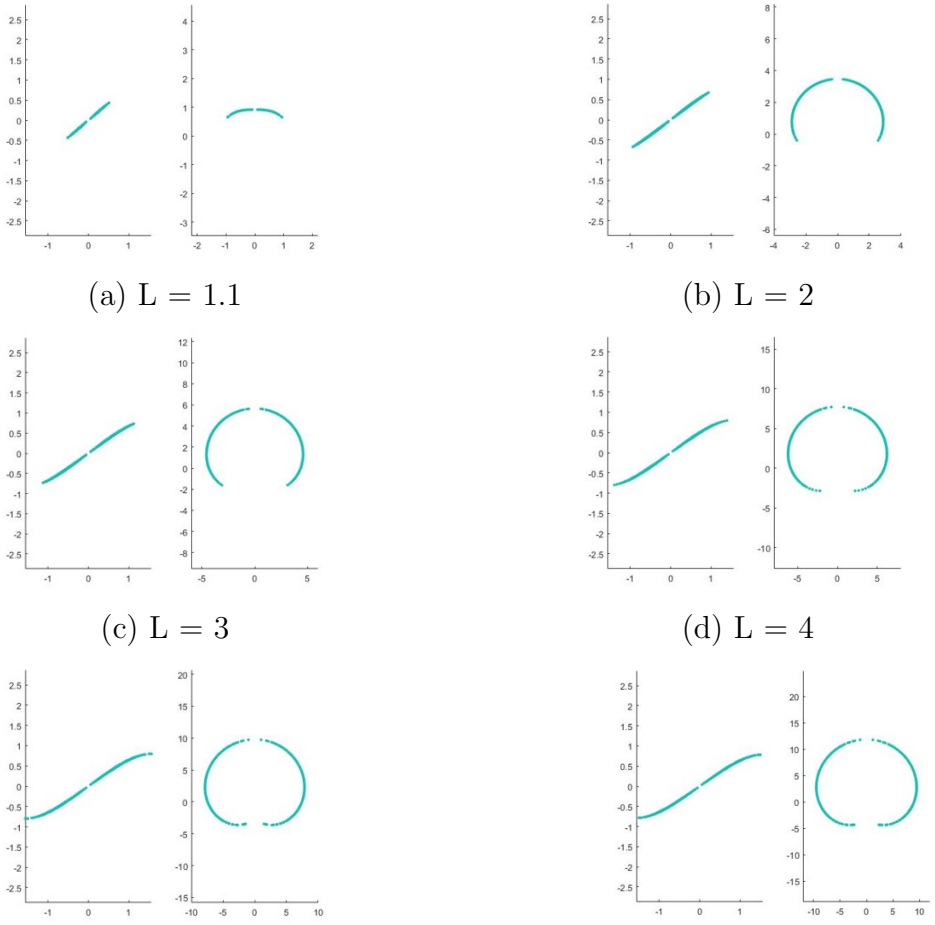

(a) L = 1.1 (b) L = 2

(c) L = 3 (d) L = 4

(e) L = 5 (f) L = 6

Figure 4.1: The wrench feasible joint configuration and workspace with different value of L when b=1, l0=0.5, k1=20, k2=30

From the figure 4.1 we can see that when $L = 1.1$ all the wrench feasible points are gathered in a short arc. Besides, we can see that different design parameters will

influence the shape and size of the WFW a lot.
In our case, we want to extract the approximate area of the WFW and we care about the time cost as well. But this method takes a lot computation time, in order to shorten the time, we improve this method by using Monte Carlo Method.

4.3.2 Monte Carlo Method

Since we want to find the injection from all the points in joint space to Cartesian space, Monte Carlo method is very suitable for our problem. Monte Carlo method is a numerical method for solving problems by means of random sampling[6]. This method is based on theory of probability and statistics. To apply Monte Carlo method to a practical problems, three steps should be followed:

(1) Define a domain of possible inputs.

(2) Generate random inputs by a meaningful probability distribution.

(3) Perform a deterministic computation of the inputs.

In our case, the domain of possible inputs is defined as the range of (θ_1, θ_2). And since our aim is to cover the full Cartesian space, the probability distribution should be not even for each point in joint space, due to the Jacobian matrix. The injection from joint space to Cartesian space is only related to the kinematic constraints, it means the result we sample in the whole joint space is the reachable workspace. To extract the wrench feasible workspace from reachable workspace, we should take into account the static equilibrium and actuating force limitation, shown in equation 3.7 and 3.1. Now, what we should do is to check if the inputs meet the two conditions and count the number of admissible inputs. By using this method, we decrease the computation consuming time a lot, which allows us to have $N = 2000000$ sample points in joint space in a reasonable time.

Chapter 5

Determine the measurement index of the wrench feasible workspace

In this chapter, several ways of determine the measurement index of the workspace are discussed. Our work will provide a theoretical basis for the parameter optimization process of the manipulator design. How can we judge if a design is a good one or bad one? If we take the parameter design process as an optimization problem, in this chapter, we are going to define its objective function. So, after generating the approximate wrench feasible workspace, our goal is to find a proper way to describe the workspace.

5.1 The number of wrench feasible sampling point

The most simple way come to our mind to measure the workspace is count its wrench feasible point configuration. As we have deduce the relationship between the joint configuration and the point cloud of WFW, which can be seen in Figure 5.1. If we have more point combinations in joint space are wrench feasible, then the point in WFW will be more.

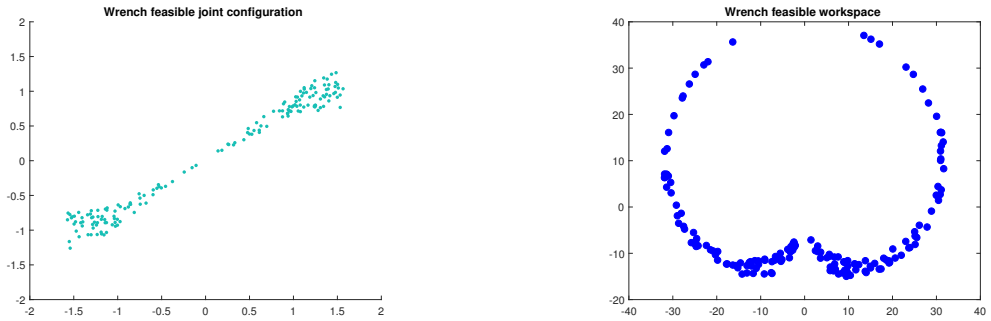

Figure 5.1: The relationship between the wrench feasible joints and WFW

We just use the method mentioned in the last chapter to realize this process. After generating N pairs of (θ_1, θ_2), and for each (θ_1, θ_2) we calculate the required force to reach this joint configuration. If the required force is in the range of actuation force, then we think this joint configuration is wrench feasible. The pseudo-code is showed as Algorithm 1.

Input: Actuation limit $[F_{1min}, F_{1max}]$ and $[F_{2min}, F_{2max}]$
Output: Number of wrench feasible sampling points *number*
use the Monte Carlo Method to generate N pairs of (θ_1, θ_2)
$number = 0$
for *each pair of* (θ_1, θ_2) **do**
  Calculate the (F_1, F_2)
  if $F_{1min} < F_1 < F_{1max}$ *and* $F_{2min} < F_2 < F_{2max}$ **then**
    $number \leftarrow number + 1$
  end
end
return *number*

Algorithm 1: Count the number of wrench feasible sampling points

We take the total number of the wrench feasible sampling points to measurement the workspace. If this number is bigger, that means the area of the joint wrench feasible space is bigger. But when we transfer from the joint space to the workspace, as we mentioned in the chapter 2, the Jacobian matrix of this mechanism is depend on the (θ_1, θ_2). From the relationship that $\triangle x = J * \triangle q$, we know that for different (θ_1, θ_2), the $\triangle x$ is different which means that the density of different area of the workspace is different. The result of the density of the workspace is showed in Figure 5.2.

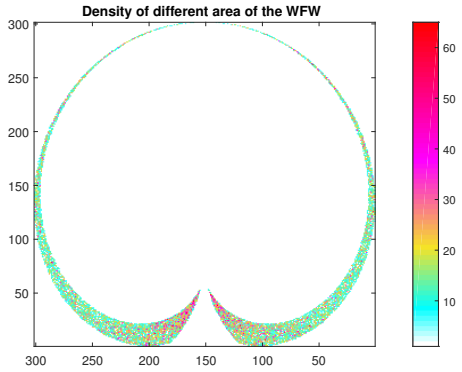

Figure 5.2: The density of different area of the workspace

From the plot of the density, we can deduce that with the same number of the wrench feasible points, if the distribution of the joints configuration is different, the area of the workspace is different. A large wrench feasible joint space doesn't mean a large

WFW. So we can not use this index to measure the quality of the workspace. In next section, we are going to measure the workspace directly.

5.2 The area of the wrench feasible workspace

In this section, we will take the area of the WFW as the measurement index. Our main idea is that, by partitioning the WFW into mesh and count the number of the bins which contain at least one point of the point cloud, which can be seen in Figure 5.3. By doing this, we can avoid the problem with the uneven distribution of the point cloud which mentioned in the last section.

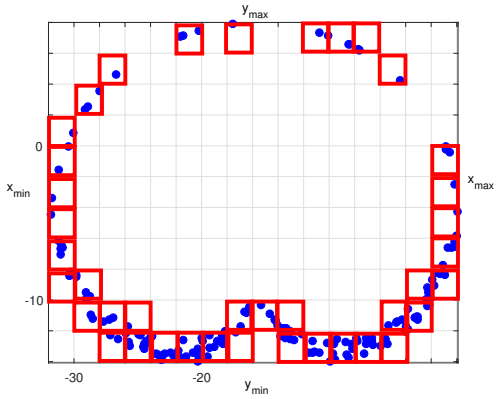

Figure 5.3: Partition the WFW to mesh

First, we introduce the partitioning fixed length mesh method. Then we found this method will be influenced by the density of the WFW. We improved this method by using adaptive mesh. To improve the accuracy, we introduce the method of depicting the edge of the WFW and fill the space inside the edge. And then we can finally get an approximate result of the area of the WFW.

5.2.1 Partitioning fixed length mesh method

The main idea of this method is that: First, we generate the imaginary mesh with fixed length according to the accuracy requirement. Then remove the extra bins based on the distribution of the point cloud. Finally, sum up the remaining bins to get the area of the required workspace. The main steps are as follow:

(1) Generate the WFW point cloud from the wrench feasible joint configuration.

(2) Create a circumscribed rectangular frame. Extract the maximum and minimum value of x and y coordinate of the WFW. Build a rectangular with the length of $x_{max} - x_{min}$ and with the width of $y_{max} - y_{min}$, and this is the circumscribed rectangular frame for the WFW.

(3) Partitioning the mesh. According to the accuracy requirement, partitioning the circumscribed rectangle frame into small sections along the x and y direction. If we choose to fix the length of the a bin as m_x and the width of m_y, so we should have the section number in the x and y direction as:

$$n_x = (x_{max} - x_{min})/m_x \tag{5.1}$$

$$n_y = (y_{max} - y_{min})/m_y \tag{5.2}$$

(4) Removal of extra bins. By using the traversal algorithm, for each point in the WFW point cloud, look for the bin that the point fall into, and increment the value of that bin. Finally, remove the bins with the value of 0, which in other words, has no point falling into this small area.

(5) Count the number of bins which contain at least one point of the point cloud n_{bin} and calculate the area of the WFW by using:

$$area_{WFW} = n_{bin} * m_x * m_y \tag{5.3}$$

Then we found that by directly using this method, when the size of the mechanism is small, this method can works well. But when the size of the mechanism grow larger, the accuracy of this method decreases a lot. This is caused by the density of the point cloud, we know from the chapter 2 that the Jacobian matrix not only depends on (θ_1, θ_2) but also depend on the size of the mechanism parameter as L and b. With the relation of the $\triangle x = J * \triangle q$, we can deduce that with the same number of sample joint configurations, when the size of the mechanism grow larger then density of the workspace will decrease, and that will generate a lot of holes in the point cloud.
We compare the result with two situation with $L = 2m$ and $L = 20m$, with the $b = 1m, l_0 = 0.5m, k_1 = 0.2N/m$ and $k_2 = 0.3N/m$, the maximum value of the actuation is $F_{max} = 100N$ and we choose the sampling point number $N = 200000$ and the length of the bin as $m_x = 0.05$ and $m_y = 0.05$. The results which can be seen in Figure 5.4.

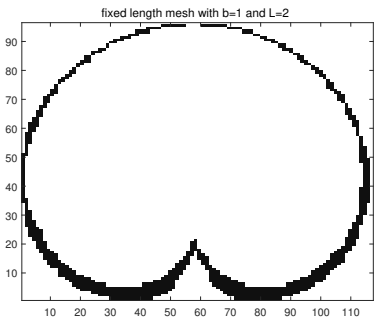

(a) case with L=2

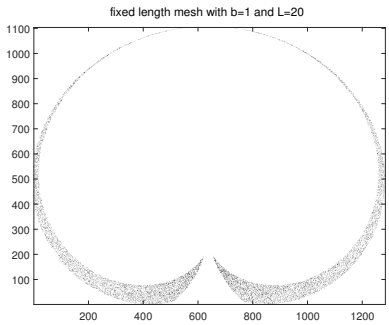

(b) case with L=20

Figure 5.4: The fixed length bins which contain at least one point

We can see from the plot that, with the mechanism of small size, the workspace is more compact so that the holes in the WFW is smaller than the bin, then all the area WFW can be taken into account. But when using this method for the mechanism of large size, the holes in the cloud point is bigger than the bin, and the result using this method can not measure the WFW anymore.
As the density of WFWs are different, when we measure this two situation with the same size of bin, we can not take the number of the bins of this two situation to compare the quality of the WFW. So we can not use the fixed length mesh to describe the area of WFW. In the next section, we will improve this method by using adaptive mesh.

5.2.2 Partitioning adaptive mesh method

Based on the adaptive mesh method of image graphic, we propose a partition adaptive mesh method to find the area of the workspace[7]. The main idea of this method is based on the partitioning fixed length mesh, but we use the mesh with adaptive length according to the size of the WFW instead of the fixed length. The main difference is that we change the idea of step (3) into:

(3) Partitioning the mesh. According to the accuracy requirement, partitioning the circumscribed rectangular frame into several sections in the x and y direction. If we suppose that we partition n_x sections in the x direction and n_y sections in the y direction, finally we will get $n * m$ meshes, with the length and the width of:

$$m_x = (x_{max} - x_{min})/n_x \tag{5.4}$$

$$m_y = (y_{max} - y_{min})/n_y \tag{5.5}$$

The pseudo code for this method is as Algorithm 2.

We test this method with two situation with $L = 2$ and $L = 20$, with the $b = 1m, l_0 = 0.5m, k_1 = 0.2N/m, k_2 = 0.3N/m$ and $F_{max} = 100N$, and we choose the sampling point number $N = 200000$ and the number of sections of the mesh in x and y directions as $n_x = 500$ and $n_y = 500$ the results which can be seen in Figure 5.5.

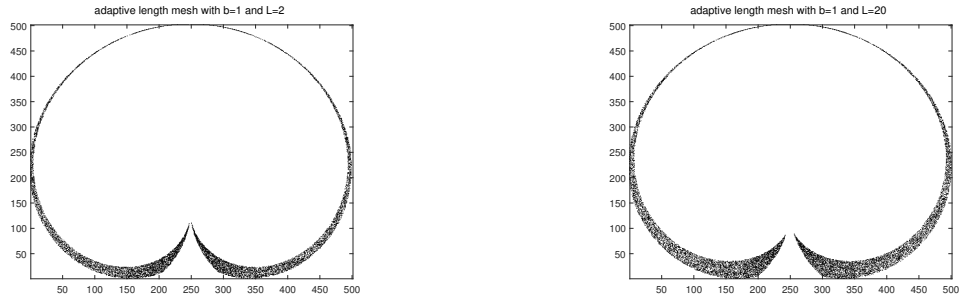

(a) case with L=2 (b) case with L=20

Figure 5.5: The adaptive length bins which contain at least one point

Input: Point cloud of WFW $P(N, 2)$; Partition number in x direction n_x and in y direction n_y

Output: The number of adaptive length bins which contain at least one point in it n_{mesh}

Extract the $x_{min}, x_{max}, y_{min}, y_{max}$ of the point cloud
$m_x = (x_{max} - x_{min})/n_x$
$m_y = (y_{max} - y_{min})/n_y$
$n_{mesh} = 0$
Build mesh as a zero matrix of size $M(n_x + 1, n_y + 1)$
for *each point of point cloud* (p_x, p_y) **do**
    $M_x = (p_y - y_{min})/m_y$
    $M_y = (p_x - x_{min})/m_x$
    $M(M_x + 1, M_y + 1) \leftarrow M(M_x + 1, M_y + 1)$
end
for *each point in mesh* $M(n_x + 1, n_y + 1)$ **do**
    if $M(i, j) \geq 1$ **then**
        $n_{mesh} \leftarrow n_{mesh} + 1$
    end
end
return n_{mesh}

Algorithm 2: Partitioning adaptive mesh method

We can see from the plot that with different size of mechanism, the density of the WFW after partitioned by the meshes stay almost the same. We increase the size of the meshes with respect to the size of the WFW, which solve the problem we have in last sub-section. But we can still see some holes in the WFW, that due to the number generating joint configuration N can not satisfy the accuracy requirement. We can solve this problem either by adding many sampling joint configurations which is time costing or by decreasing the accuracy, which in other words, partitioning less sections in the x and y direction. So in the next section, we will improve this method to satisfy the high accuracy requirement with low sampling ratio.

5.2.3 Depicting boundary curve

In this section, we will depict the boundary[8] of the WFW. Based on the method of partitioning the WFW with adaptive meshes. We already know the approximate scope of the workspace. Then we will try to find its vertical boundary and lateral boundary. To find the lateral edge, we have already partition the y direction of the WFW to n_y sections, so we will scan each row of the meshes, to find the maximum value and the minimum value. If we consider the whole WFW, the detection of the lateral edge is complex as there are many small areas and as the mechanism is vertical symmetric, so we just take the left half of the WFW for boundary detection.
There are three situations which we focus on, as showed in Figure 5.6. When we

detect the edge on the row AA', we only need to detect two bins, which are the bins with maximum column and minimum column. And for the column BB', we need to detect 4 edge points, as there is a hole in the WFW. For the column CC', we need to detect 3 points, one of which is a vertex of the WFW and the other two are the edge points. In order to deal with this three situations, we use the process as follow:

(1) For each row, detect the bins with maximum and minimum column, we mark them with red.

(2) Calculate the difference between the two red bins.

(3) If the difference is smaller than the given threshold, we think this is the situation same as AA'. If the difference is larger than the given threshold, then go to step 4.

(4) We take the middle bin of the two red bins. Then we check if the value of middle bin is greater than 0, which means there should have at least one point fallen into this bin. If true, then the middle bin is located in the WFW, we take it as the situation AA'. If not, then this situation should belong to the situation of BB' or CC', we go to step 5.

(5) We divide each row into two search ranges by the middle bin. For the left area, the outer edge should be the red bin with the minimum column and the inner edge should be the purple bin with the maximum value in the range of $[1, middle]$. And for the right area, the outer edge is the red bin with the maximum column value and the inner edge should be the purple bin with the maximum value in the range of $[middle + 1, n_y]$. So if in the situation of BB', then we should detect four bins and if in the situation of CC', then one purple bin coincides one red bin, we will detect three bins.

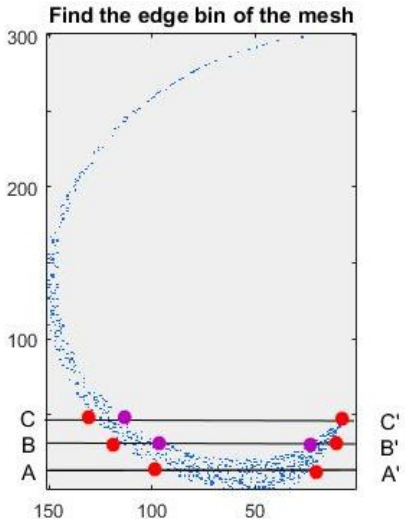

Figure 5.6: Find the edge bins of the WFW

We use the same method to find the vertical boundary. So finally we can deduce the boundary in the x and y direction. And by adding them up, we can finally get

the total edge of the WFW. We tried the case with the parameter as $b = 1m, L = 20m, k_1 = 0.2N/m, k_2 = 0.3N/m, F_{max} = 100N, N = 200000$ and $n_x = 500, n_y = 500$. For the threshold to check the middle bin, we set $threshold = n_y/5$, the result is showed in Figure 5.7.

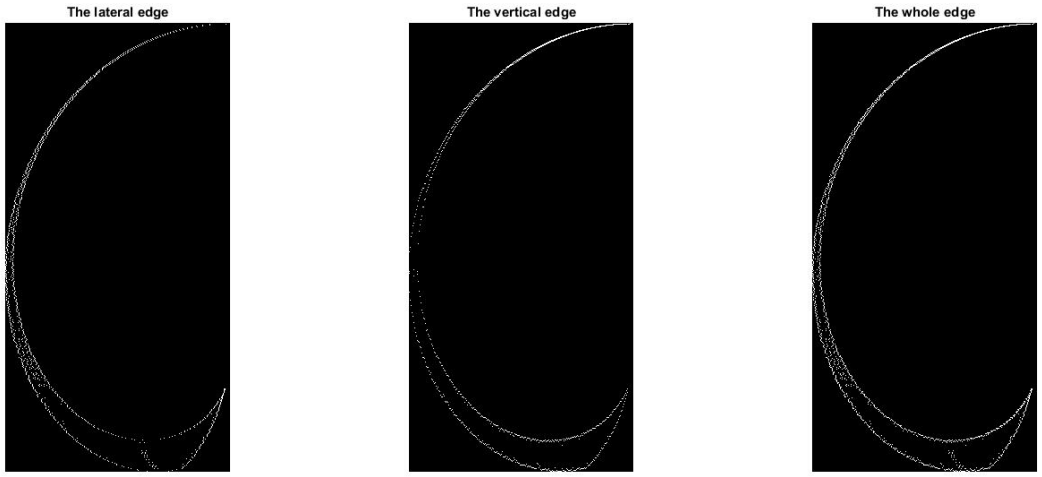

(a) The lateral edge (b) The vertical edge (c) The whole edge

Figure 5.7: The edge bins of the wrench feasible workspace

5.2.4 Fill the WFW and calculate the area

After extract the edge of the WFW, we will fill the WFW by the vertical and the lateral edge. To fill the area by vertical edge, we will follow the following steps:

(1) For every row of the vertical edge matrix, search for the bin with value greater than 0, put them in the array $edgey$;

(2) If the number of the bins is 4, then it is the situation BB', we set the bins of the column between $[edgy(3), edgy(4)]$ and $[edgy(1), edgy(2)]$ to 1.

(3) If the number of the bins is 3, then it is the situation of CC', we set the bins of the column between $[edgy(1), edgy(2)]$ to 1.

(4) If the number of the bins is 2, then it is may be the situation AA', or two isolate points. We need to check the difference between $edgy(1)$ and $edgy(2)$, if the difference is smaller than $n_y/2$, then it is the situation of AA', we set the bins of the column between $[edgy(1), edgy(2)]$ to 1. Otherwise we will check the value of the middle bin in mesh matrix, if greater than 0, then it is the situation of $'AA'$. If not, we will not fill the column between $[edgy(1), edgy(2)]$.

We use the same method to fill the area using the vertical edge, and then we add them up to get the whole area fill. We fill the area by using the edges showed in Figure 5.7, and then we get the result as showed in Figure 5.8.

(a)Fill WFW by lateral edge(b)Fill WFW by vertical edge (c)The whole area

Figure 5.8: The edge bins of the wrench feasible workspace

We can compare with the result by using partitioning adaptive mesh with the same generating joint configurations number as $N = 200000$ and the partitioning accuracy as $n_x = 500$ and $n_y = 500$, which can be seen in Figure 5.9.

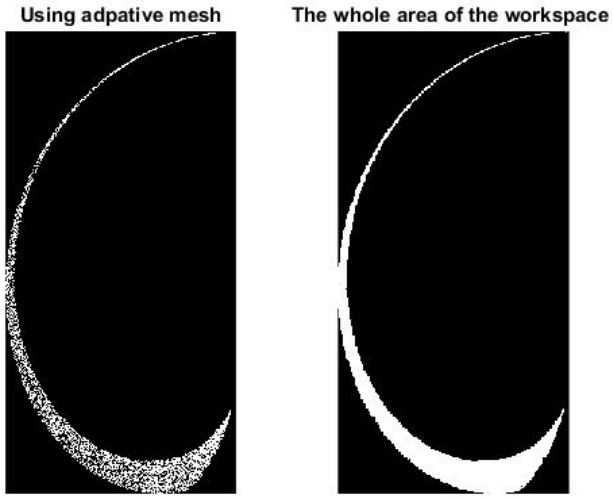

Figure 5.9: Comparison of the result by using partitioning adaptive mesh method and the result after fill the WFW by edge

From the result we can see that, after improve the partitioning adaptive mesh method by filling the WFW by edge, we solve the problem causing by the density of the WFW. To calculate the area of the WFW, we scan the matrix of the filled area, and count the number of bins with the value greater than 0 as n_{fill} and then we calculate the

area by Equation 5.6.

$$Area = n_{fill} * m_x * m_y \tag{5.6}$$

By using this method, we can finally deduce the approximate value of the area of the WFW.

5.3 The shape of the area

From the chapter 4 we can see that, the parameter of the mechanism not only influence the size of the WFW but also the shape of the WFW. From the previous method, we can find that with the same shape of the WFW, the area will always be larger when the size of the mechanism is larger as the size of the little bin will be influenced by the value of $x_{max} - x_{min}$ and the value of $y_{max} - y_{min}$. We don't want to have a big area of the WFW with the cost of building a very huge mechanism. We just want to have the optimized shape of the WFW with a compact and reasonable size of the mechanism.
How to describe the shape of the WFW? If we just use the method mentioned above by counting the number of the filled bins instead of calculating the area, to find out the ratio between the filled area and area of circumscribed rectangle of the WFW. We will find the (a) case of Figure 4.1 have the maximum value. As the WFW is a very small arc, so the WFW is more compact and the density of the filled area is high.
So we improve method above by finding the range of the reachable workspace instead of finding the range of the WFW and then make the partitioning, finding the edge and filling the WFW. Then we count the number of filled bins. As we partitioning the reachable workspace with the same total number of bins as $n_x * n_y$, if we divide the number of filled bins by the total number of bins, the result can be seen as the ratio between the WFW area (the yellow area) and the area of circumscribed rectangle of reachable workspace (the red area),where the reachable workspace is the blue area, which is showed in the Figure 5.10.

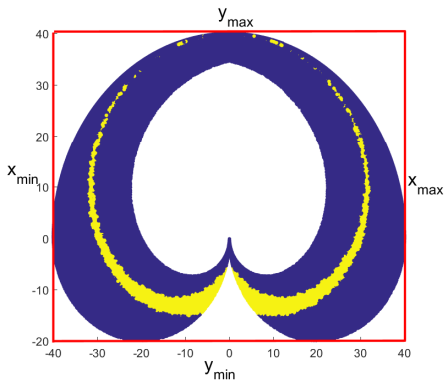

Figure 5.10: The relationship between the circumscribed rectangular of the reachable workspace and the WFW

Chapter 6

The relationship between the design parameters and the wrench feasible workspace

In this chapter, we will discuss the influence of the design parameters of the mechanism on the shape of the WFW which is described by the ratio between the area of WFW and circumscribed rectangle of reachable workspace. We choose the generating number of N as $N = 2000000$ and we divide the section in the x and y direction of the circumscribed rectangular of the reachable workspace as $n_x = 500$ and $n_y = 500$.

6.1 The influence of the length of the mechanism

First, we will discuss about the influence of the ratio L/b on the WFW's shape. We traverse ratio L/b from $[1.1, 20]$, and we use the method we mentioned in the last chapter to calculate the ratio between the area of the WFW and the area of the circumscribed rectangular of RW. We fix $b = 1m, k_1 = 0.2N/m, k_2 = 0.3N/m, F_{max} = 100N$ and $l_0 = 0.1m$. The result can be seen from the Figure 6.1.

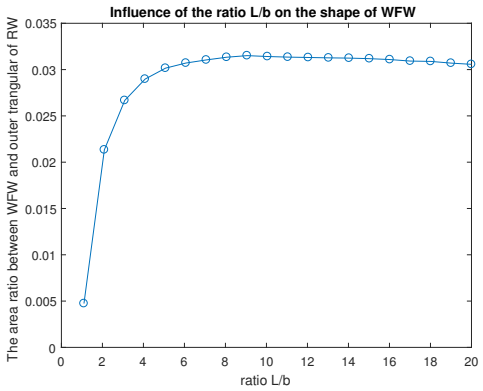

Figure 6.1: The influence of the ratio L over b on the shape of the WFW

We can see from the plot that, at first the area of WFW grows larger, then converges to a constant value and remains stable. At the beginning, the shape of WFW is a short arc which only occupy a very small part of the circumscribe rectangle of RW. During the ascending phase, as L increases,the shape of WFW grows larger. When L increases to $6m$, the shape begin to decrease slowly, as for the mechanism with large L, to reach for the same joint position of θ_1, θ_2, we need to extend the spring longer, which will need more force.

From the chapter 2, we know that l_0 should always smaller than $L-b$, so we fixed the $b = 1m, L = 10m$ and with $k_1 = 0.2N/m, k_2 = 0.3N/m, Fmax = 100N$ and traverse ratio $l0/b$ from $[0.1, 9]$. The result can be seen from the Figure 6.2.

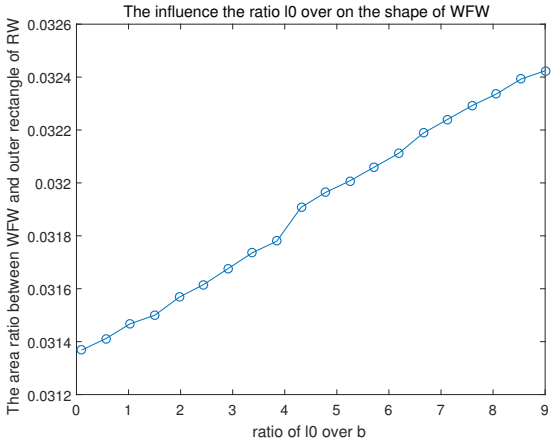

Figure 6.2: The influence of the ratio l0 over b on the shape of the WFW

As the original length of spring l_0 increases, the required force to driven the mechanism to the same configuration is decreased, so the shape of WFW becomes larger.

6.2 The influence of the spring stiffness

First, we fix the ratio between k_2 and k_1 as 3/2, and we traverse the total stiffness of the spring as $k = k_1 + k_2$ from $[10N/m, 50N/m]$,with $b = 1m, L = 10m, l0 = 0.5m, F_{max} = 100N$, the result can be seen in the Figure 6.3.

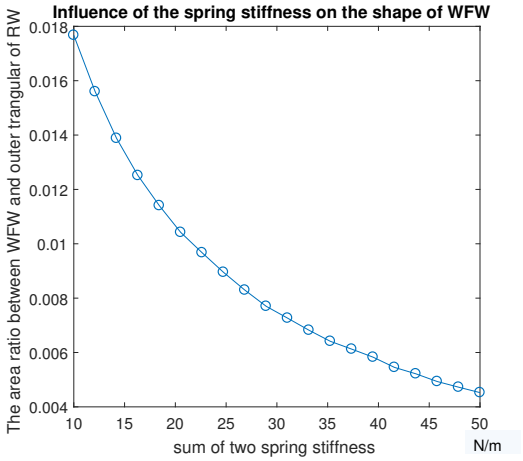

Figure 6.3: The influence of the $k_1 + k_2$ on the shape of the WFW

The result is obviously reasonable. Because as the stiffness k_1 and k_2 increase, we need more force to reach for the same joint position θ_1, θ_2 than before . The shape of WFW will becomes thiner and smaller. Then, we fixed one of the stiffness and change ratio between the two stiffness. The result can be seen in Figure 6.4

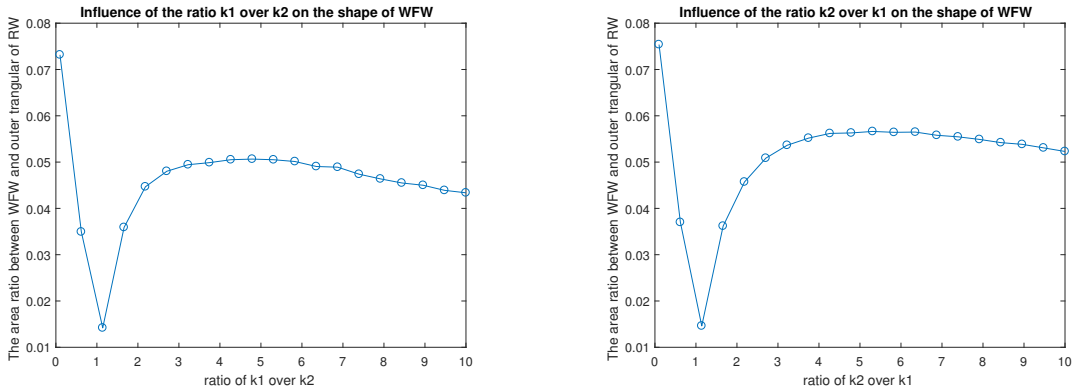

(a)ratio of k1 over k2 when k2 = 0.3 (b)ratio of k2 over k1 when k1 =0.2

Figure 6.4: The influence of the ratio between k1 and k2 on the shape of the WFW

We can see that the shape of these two plots looks like the same. We can not find a proper ratio between the k_1 and k_2 to maximize the WFW shape. When one of the spring stiffness is very small the WFW is big. Since we don't consider the stiffness of

the whole mechanism, we have no constraint for the spring stiffness. Normally, when one of the stiffness increases, the area of WFW should decrease gradually. But when $k_1 = k_2$, from the equation 3.7 and 3.8, we know that the area is always equals to 0. Then, the area increase to normal value and decrease gradually.

6.3 The maximum actuator force

Then we test the case with $L = 10m, b = 1m, l_0 = 0,5m, k_1 = 0.2N/m, k_2 = 0.3N/m$ then we traverse the maximum value of the maximum actuator force F_{max} from $[50N, 5000N]$, the result can be seen in the Figure 6.5.

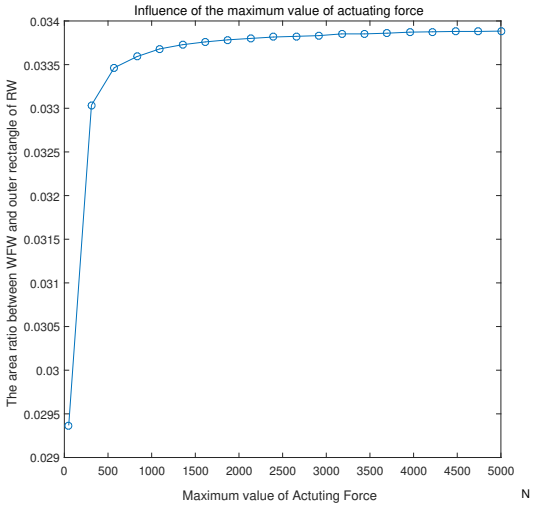

Figure 6.5: The influence of the Fmax on the shape of the WFW

We can see from the plot that, with F grow bigger, at first the shape of the WFW grow bigger, which is obvious that with larger force, we can reach more points in the workspace. But the maximum WFW for a given mechanism is its reachable workspace, we can not have the shape of the WFW always grow by using larger actuation force. For a given mechanism, we can find an optimal value of F_{max}.

Chapter 7

Conclusion

In this report, based on the known kinematic model and actuation strategy, we introduce the method to generate and to measure the wrench feasible workspace for a 2-dof tensegrity manipulator. We improve the discretization method with Monte Carlo method to generate the joint configurations from the total joint space, which improve the speed of calculation a lot. Then in the process of measurement of the WFW, we introduce several ways to measure the WFW. Finally, we came up with the method to calculate the ratio between the area of the WFW and the circumscribe rectangle of the reachable workspace to measure the shape of the WFW.
The advantage of this method is that it can guarantee high calculation accuracy in a reasonable calculation time. And compared with the other method we mentioned above, it can eliminate the influence of uneven distribution of the point cloud, the influence of the density of WFW and the influence of the size of the mechanism. But it has also the disadvantage as, this can only work for the case when the WFW is thick and has a real area. For our case, when the stiffness of the spring is very big, and the thickness of WFW can be very small like a line. In this case, we can not have a good measure of the WFW and it will always by influenced by the density of the edge bins. As shown in figure 7.1 with $b = 1m, L = 4m, l0 = 0.5m, k1 = 20N/m, k2 = 30N/m$.

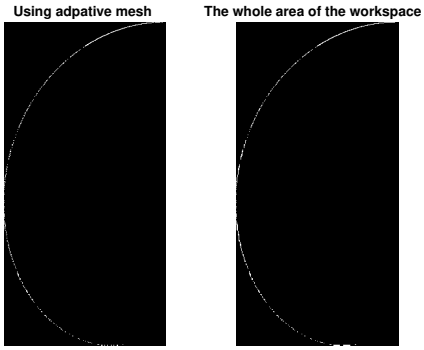

Figure 7.1: The failed circumstance

At this stage, we don't take the gravity into account, as we consider the manipulator as a horizontal manipulator. In the next step, we will take the gravity of the mechanism into account and then we will have some constraints on the stiffness of the mechanism. We will only take into the equilibrium point with the stiffness greater than 0 as the stable equilibrium point. In that case, we will have some new limits on the stiffness of the spring and the size of the mechanism. After we deduce the relationship between the design parameter and the shape of the WFW, we can choose the proper design variables and define the optimization problem.

Bibliography

[1] A. van Riesen, P. Wenger, C. Chevallereau, Analysis of a tensegrity mechanism inspired from a bird neck.

[2] M. Furet, M. Lettl, P. Wenger, Kinematic analysis of planar tensegrity 2-X manipulators.

[3] A. van Riesen, M. Furet, C. Chevallereau, P. Wenger, Dynamic analysis and control of an antagonistically actuated tensegrity mechanism.

[4] P. Wenger, D. Chable, Kinetostatic Analysis and Solution Classification of a Planar Tensegrity Mechanism, proc. 7th. Int. Workshop on Comp. Kinematics, Springer, ISBN 978-3-319-60867-9, pp422-431,2017.

[5] Q. Boehler, I. Charpentier, M. Vedrines, P. Renaud, Definition and Computation of Tensegrity Mechanism Workspace.

[6] J. Rastegar, B. Fardanesh, manipulator workspace analysis using the Monte Carlo method, Mech. Mach. Theory Vol. 25, No.2, pp. 233-239, 1990.

[7] H. Tian, H. Ma, J. Wei, Workspace and Structural Parameters Analysis for Manipulator of Serial Robot.

[8] Y. Cao, S. Qi, K. Lu, Y. Zang, G. Yang, Shape and Size Computation of Planar Robot Workspace, World Congress on Computer Science and Information Engineering,2009.